Multiscale analysis of precipitable water vapor over Africa from GPS data and ECMWF analyses

Olivier Bock, Francoise Guichard, Serge Janicot, Jean-Philippe Lafore, Marie-Noëlle Bouin, Benjamin Sultan

Multiscale analysis of precipitable water vapor over Africa from GPS data and ECMWF analyses

O. Bock,[1] F. Guichard,[2] S. Janicot,[3] J. P. Lafore,[2] M.-N. Bouin,[4] and B. Sultan[3]

Received 12 September 2006; revised 19 February 2007; accepted 6 April 2007; published 9 May 2007.

[1] This is the first climatological analysis of precipitable water vapor (PWV) from GPS data over Africa. The data reveal significant modulations and variability in PWV over a broad range of temporal scales. GPS PWV estimates are compared to ECMWF reanalysis ERA40. Both datasets show good agreement at the larger scales (seasonal cycle and inter-annual variability), driven by large scale moisture transport. At intra-seasonal (15–40 days) and synoptic (3–10 days) scales, strong PWV modulations are observed from GPS, consistently with ECMWF analysis. They are shown to be correlated with convection and the passage of equatorial waves and African Easterly waves. The high-frequency GPS observations also reveal a significant diurnal cycle in PWV, which magnitude and spectral content depends strongly on geographic location and shows a seasonal modulation. The diurnal cycle of PWV is poorly represented in ERA40 reflecting weaknesses in the water cycle of global circulation models at this timescale. **Citation:** Bock, O., F. Guichard, S. Janicot, J. P. Lafore, M.-N. Bouin, and B. Sultan (2007), Multiscale analysis of precipitable water vapor over Africa from GPS data and ECMWF analyses, *Geophys. Res. Lett.*, *34*, L09705, doi:10.1029/2006GL028039.

1. Introduction

[2] Atmospheric water vapor is a key variable of the global climate system and hydrologic cycle. It shows significant variability, both in space and time over a large range of scales, resulting from interactions between atmospheric, land and ocean processes. Precipitable water vapor (PWV) is a good indicator of the variability of water vapor in the lower troposphere and related processes. In terms of water budget, it represents the tendency of water vapor storage in the column of atmosphere, as a result of the balance between precipitation, evaporation and convergence of humidity [*Fontaine et al.*, 2003]. In the present work, we analyze PWV variability with the help of Global Positioning System (GPS) observations, from a network of ground-based receivers in Africa (Figure 1), and the 40-year (ERA40) re-analyses from European Centre for Medium-Range Weather Forecasts (ECMWF) [*Simmons and Gibson*, 2000]. The GPS dataset consists in a combined zenith tropospheric delay (ZTD) product from the International GNSS Service [*Gendt*, 2004]. ZTD estimates are converted into PWV [*Bevis et al.*, 1994] using surface pressure and 2-m temperature from ERA40 for all stations except Dakar where data from ECMWF operational analysis were used instead (this station operated only from mid 2003 on). Since the conversion is not very sensitive to the surface parameters [*Bevis et al.*, 1994] and GPS data are not assimilated into ERA40, GPS PWV allows for an independent validation of ERA40. The GPS PWV data are representative of a spatial scale of 20–50 km in the troposphere (assuming, e.g., observations down to 5° elevation and a water vapor scale height of 2–5 km). This is of similar, though slightly higher, resolution than the ERA40 dataset (the latter having a horizontal resolution of ~125 km). We refer to *Bock et al.* [2007] for further description of these datasets. In the present letter, we present climatic features at four of these African stations.

2. Seasonal Cycle and Inter-Annual Variability

[3] The seasonal cycle in PWV observed in the tropics is a result of large-scale processes. It mainly reflects the migration of the inter-tropical convergence zone (ITCZ) from one hemisphere into the other, following the movement of maximum solar heating with a lag of about 6 weeks. Figure 2 shows the PWV seasonal cycle from GPS and ERA40 at four GPS stations located in contrasted regions of Africa for which the available time series were the longest. Nevertheless, the periods of time are unequal between them (see legend of Figure 2). The agreement between GPS and ERA40 is generally good. These stations have marked but different seasonal cycles. At the northernmost station (Mas Palomas; Figure 2a), the magnitude of PWV excursion throughout the year (12 kg m^{-2}) and the average PWV (20 kg m^{-2}) are relatively small, but their ratio is quite strong (60%), reflecting a marked seasonal cycle. The inter-annual variability for each month (lower part of the plot) is quite small at this station (standard deviation about 2 kg m^{-2}). At station Dakar (Figure 2b) the seasonal cycle is very pronounced. The average value and excursion throughout the year are both about 30 kg m^{-2}, i.e., a seasonal modulation of 100% and a ratio of highest over lowest monthly value of ~3. PWV shows a slow and regular increase between March and August, while the decrease is much faster, between September and November. The highest values are observed during the monsoon season and may be due to large moisture fluxes from the south-west in the lower troposphere and from the north-east in the middle troposphere as well as vertical transport due to convection and evaporation [*Fontaine et al.*, 2003; *Sultan*

[1]Institute Pierre-Simon Laplace, Service Aeronomie du CNRS, Université Paris VI, Paris, France.
[2]Groupe de Météorologie de Moyenne Echelle, Centre National de Recherches Météorologiques, Météo-France, Toulouse, France.
[3]Institute Pierre-Simon Laplace, Laboratoire d'Océanographie et du Climat, Université Paris VI, Paris, France.
[4]Laboratoire de Recherches en Géodésie, Institut Géographique National, Marine la Vallee, France.

0094-8276/07/2006GL028039

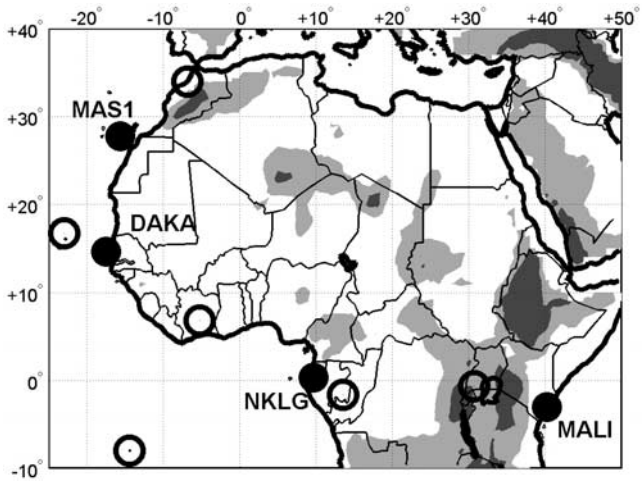

Figure 1. Map of the region of interest with the GPS stations used in this study (black filled circles): MAS1 (Mas Palomas, Gran Canaria, Spain), DAKA (Dakar, Sénégal), NKLG (N'Koltang, Gabon), and MALI (Malindi, Kenya). Other African GPS stations existing in the region are indicated as open circles. Ground elevation is indicated as grey shading (600 m as light grey and 1200 m as dark grey).

et al., 2003; *Matthews*, 2004]. The inter-annual variability has one marked peak in December–January that might be linked to large scale dry and wet air intrusions. Station N'Koltang (Figure 2c) and Malindi (Figure 2d) are located near the equator. Both exhibit a double peak in PWV, in April–May and October–November, which traces the passage of the ITCZ. Both have moderate to small seasonal cycle (20% at N'Koltang and 34% at Malindi). The inter-annual variability at N'Koltang is very small while it is very marked at Malindi during the boreal winter months. At the latter, the standard deviation reaches 7–9 kg m^{-2} according to ERA40 and 3–5 kg m^{-2} according to GPS. This variability may be linked to the El Niño Southern Oscillation as suggested by the correlation observed between GPS PWV monthly-mean anomaly with the Niño-3 index (http://www.cdc.noaa.gov) for the period 1997–2005. Similar correlations have been reported by *Wagner et al.* [2005].

3. Intra-Seasonal Timescale

[4] Intra-seasonal time-scales are influenced by a broad range of processes, ranging from synoptic to global disturbances down to Mesoscale Convective Systems (MCSs). These processes have been shown to impact on precipitation, convection and atmospheric circulation [*Diedhiou et al.*, 1999; *Wheeler and Kiladis*, 1999; *Sultan et al.*, 2003; *Matthews*, 2004]. Whether they have a signature in PWV remains unknown. This question is addressed here from the analysis of GPS and ERA40 PWV data at Dakar for the period from September 2003 to July 2004. Figure 3a shows the PWV time series from both datasets and demonstrates good accordance (7.5% RMS difference and r = 0.99 correlation coefficient). A large variability in PWV is observed at Dakar, with more low frequencies during winter and more high frequencies during summer. Figure 3b shows a wavelet diagram of the ECMWF PWV data, which helps

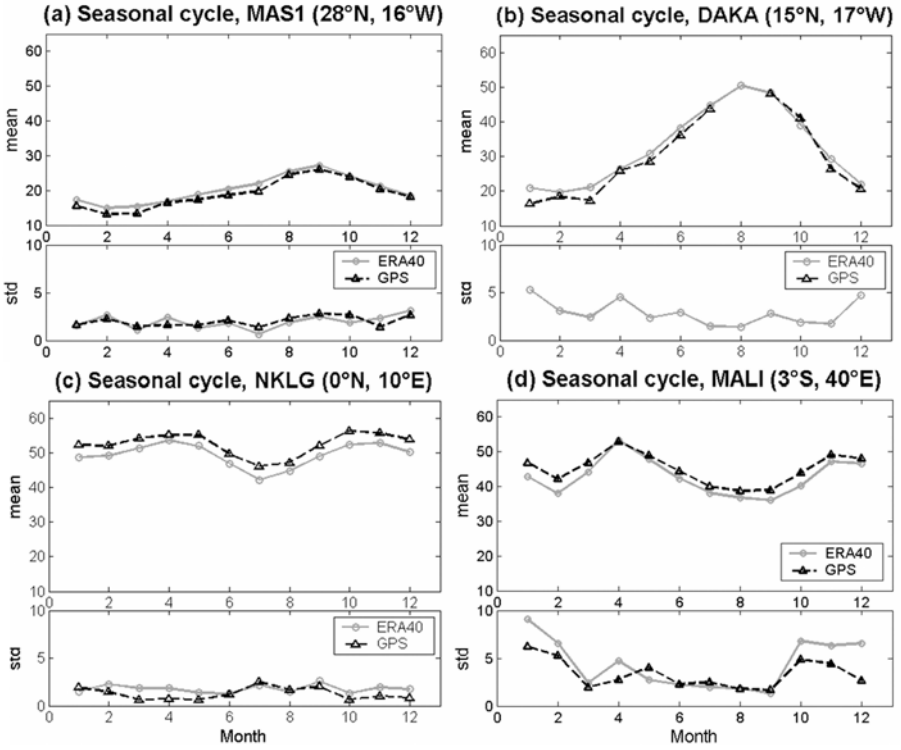

Figure 2. (top) Monthly mean and (bottom) standard deviation of PWV from GPS (black dashed lines with triangles) and ERA40 (gray solid lines with circles), at four GPS stations. Horizontal time axis unit is month. Vertical axis unit is kg m^{-2}. Data from ERA40 cover the period 1997–2002; and GPS the period 1997–2004 for stations MAS1 and MALI, 2000–2004 for NKLG, and mid 2003–mid 2004 for DAKA.

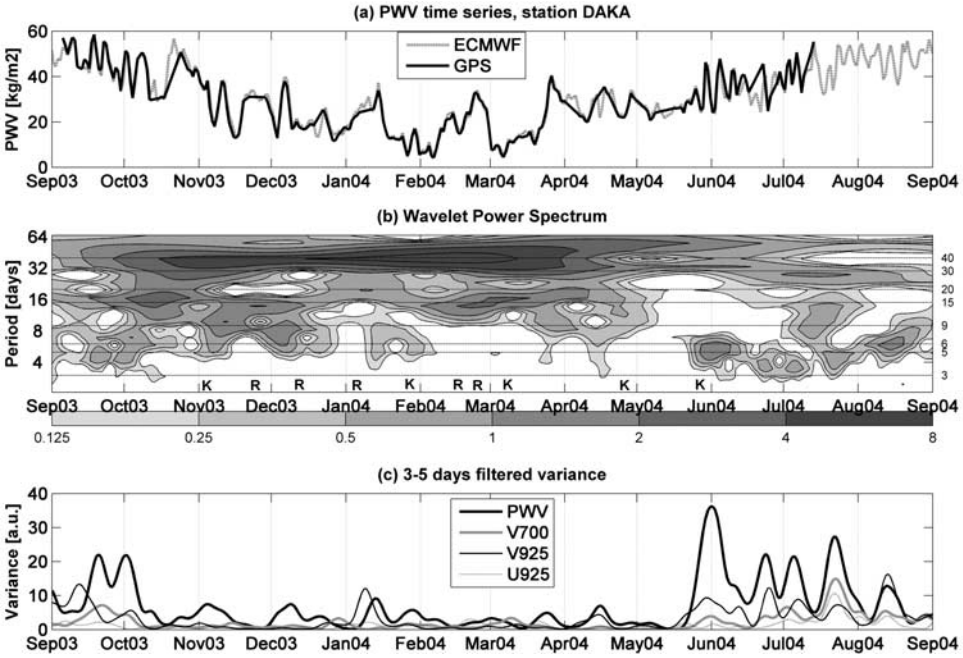

Figure 3. Intra-seasonal analysis at station DAKA: (a) PWV time-series from GPS (black line) and ECMWF (gray line); (b) wavelet spectrum of GPS PWV, with amplitude shown as gray shading (arbitrary unit) and letters at bottom indicating the passage of Kelvin (K) and Rossby (R) waves; and (c) 3–5 days filtered variance of PWV and wind components from ECMWF (see legend inset and text).

identifying the dominant periodicities [*Diedhiou et al.*, 1999]. A strong signal is seen at the 40-day period during fall and winter, which is peaking in February 2004 (three cycles of this signal can be distinguished in Figure 3a). It is coincident with a peak in 925 hPa zonal wind at Dakar (not shown). Inspection of convection and Madden-Julian Oscillation (MJO) diagnostics available at the Climate Diagnostic Center (CDC, http://www.cdc.noaa.gov) indicate that this signal is in phase with convection observed over Dakar and in phase opposition with convection over the maritime continent where the MJO signal is peaking. This suggests some remote connection between MJO events and convection over Africa such as discussed by *Matthews*, 2004. MJO events are generally accompanied by equatorial waves. We thus used CDC convection diagnostics (based on work by *Wheeler and Kiladis* [1999]) to detect Rossby and Kelvin waves, which are indicated as R and K, respectively, in Figure 3b. Waves are mainly detected during the dry season (between November 2003 and June 2004). They most often coincide with PWV maxima in the 15–25 day periodicity band for Rossby waves and 5–10 day band for Kelvin waves.

[5] African Easterly Waves (AEWs) occur mostly during the summer and have typical periodicities in the 3–5 and 6–9 day bands [*Diedhiou et al.*, 1999]. PWV fluctuations show significant energy in these periodicity bands (Figure 3b). In order to detect 3–5 day AEWs, we inspected filtered PWV and dynamical fields from ECMWF analyses (Figure 3c). The strongest occurrences in this period band happen during the monsoon season. Large PWV peaks are associated with peaks in all three wind components displayed. During summer 2004, the correlation coefficient is r = 0.56 and r = 0.64 between PWV and the meridional wind component at 700 and 925 hPa (V700 and V925), respectively, and r = 0.42 between PWV and the zonal wind component at 925 hPa (U925). These numbers and the plot in Figure 3c suggest a strong interaction between the monsoon flow, AEWs and the total column water vapor. The correlation coefficients, calculated only for the 2004 summer data where the variance of V700 exceeds a threshold of 4 m^2/s^2 become r = 0.76, 0.23, and 0.66, respectively. These suggest further that in the presence of AEWs, significant modulations in the water vapor transport occur from modulation of the V700 and U925 wind components. The impact of these modulations on the precipitation efficiency over the central Sahel must be investigated more precisely.

4. Seasonal Variations of the Diurnal Cycle

[6] The diurnal cycle is one of the fundamental modes of variability in the global climate [*Yang and Slingo*, 2001]. It is associated with large and well-defined variations in solar forcing, inducing diurnal (24 h) and semi-diurnal (12 h) oscillations, denoted S_1 and S_2, respectively. The tropics exhibit a marked diurnal cycle in convection, precipitation, high cloud cover, and humidification of the upper atmosphere, with significant time lags between these parameters [*Tian et al.*, 2004]. However, the diurnal variation of PWV remains largely unknown. It is illustrated here at the four GPS stations already considered in section 2. Figure 4 shows monthly means (filled contours) and sub-monthly variability (standard deviation plotted as dotted contours) of PWV diurnal anomalies. This representation allows for discussing the seasonal variation of the diurnal cycle's magnitude and, to some extend, makes the link between different timescales.

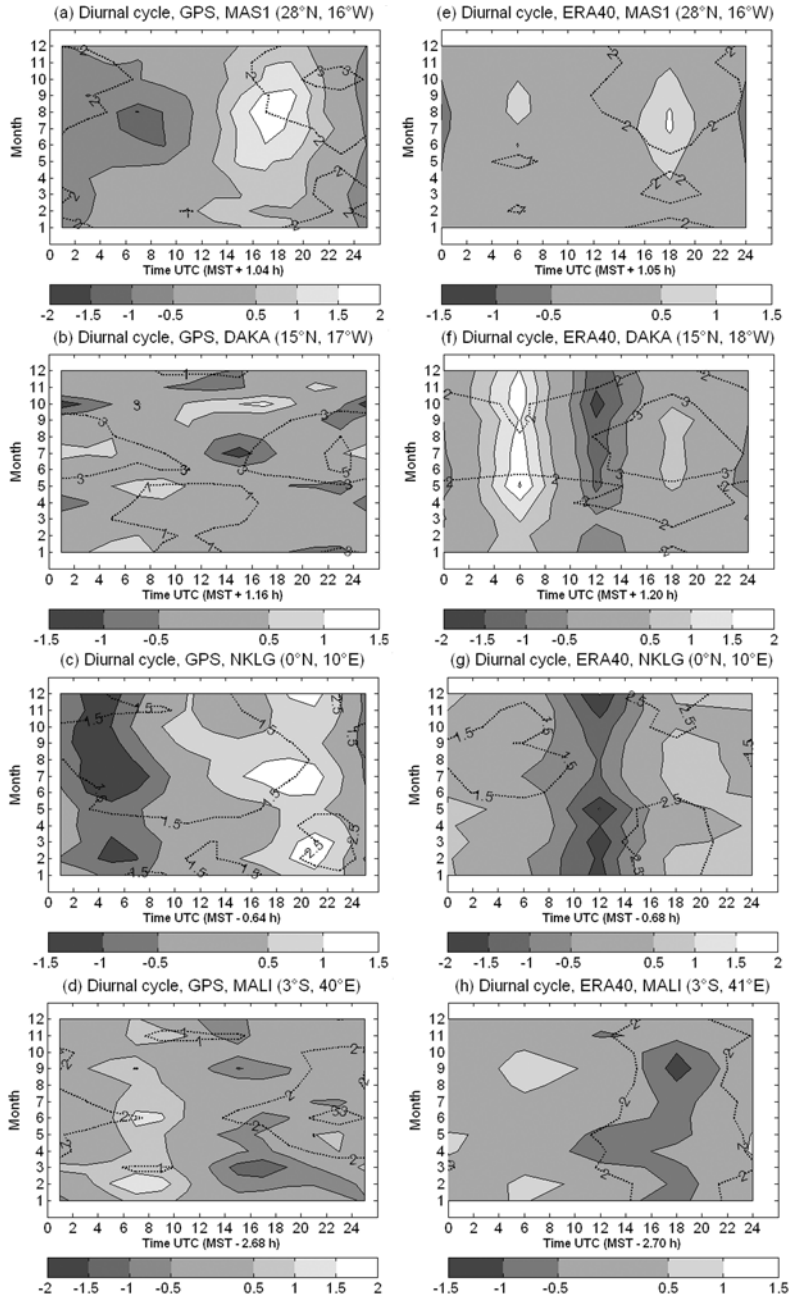

Figure 4. Seasonal variation of PWV diurnal cycle anomalies at the same four stations and periods as in Figure 2: (a–d) GPS data and (e–h) ERA40. Gray shading shows monthly averages (see color bar at bottom of each plot) and dotted contour lines show the sub-monthly standard deviation (1 kg m^{-2} interval). Horizontal axis is hour in day (UTC), vertical axis is month of year. Time shift between UTC and mean solar time (MST) is indicated at the bottom of each plot.

[7] Station Mas Palomas (Figure 4a) has a marked diurnal cycle, with a dominant S_1 oscillation. The maximum is located in the afternoon between 16 and 18 UTC (15 and 17 local time, LT) and the minimum during nighttime between 01 and 08 UTC (00 and 07 LT). The magnitude of the peaks is the strongest during summer (June–September), where it reaches -1.5 to $+2$ kg m^{-2}. This large magnitude might be due to local breeze circulations. The variability of the diurnal cycle is the strongest in the evening around 23 UTC (22 LT). This might be linked to the diurnal cycle of convection, which also exhibits a maximum in the evening [*Tian et al.*, 2004]. Compared to GPS, ERA40 PWV diurnal cycle at this station is not well sampled and/or represented in the model. The model exhibits a double peak, with maxima at 06 and 18 UTC (i.e. ~05 and 17 LT) during the summer months (Figure 4e). The latter is the strongest, which is consistent with the GPS, but the former indicates that some of the processes interact with a S_2 periodicity while they should not. Similar to GPS, the variability is the strongest in the evening, which is likely to reflect

strong convective activity. With such a monthly mean diagnostic, station Dakar does not exhibit a strong and coherent diurnal cycle in PWV (Figure 4b). This is partly linked to the fact that only a small signal comes out from the monthly averages. The standard deviation contours indicate that the variability is strong during the summer months (May to September). Inspection of time series (see Figure 3a) shows that PWV variability is especially intense (5–10 kg m^{-2}) at timescales of a few days. The fact that these large variations are significantly damped by the diurnal cycle averaging suggests that there is no simple link between the diurnal cycles of meso- and synoptic-scale processes at this location and scale. This difference could be linked to the more propagative nature of the former and the more local interactions in the vertical column of the latter. Similar to Mas Palomas, Dakar has strongest PWV variability in the evening and during nighttime. In contrast to GPS, the ECMWF diurnal cycle at this station is strong, with a +2 kg m^{-2} maximum at 06 UTC (~5 LT) and a −1.5 kg m^{-2} minimum at 12 UTC (~11 LT), see Figure 4f. Such a behavior is more representative of ocean processes than continental ones [*Tian et al.*, 2004]. A secondary maximum (minimum) can also be seen at 18 UTC (00 UTC) during the summer months. Similar to the previous site, the variability is stronger in the evening. Station N'Koltang has a marked diurnal cycle, with maxima of ±1.5 kg m^{-2} (Figure 4c). Average PWV is peaking in the evening around 21 UTC (~20 LT) throughout the year, with smaller values in spring and autumn. A secondary peak is seen at 11 UTC (~10 LT) between August and December. Variability is larger during the heavy rain season (November–April), possibly linked to interactions with convection (e.g., vertical moisture transport) and precipitation (e.g., evaporation of hydrometeors). The evening maximum in PWV is quite correctly reproduced by ERA40 (Figure 4g), but neither the minimum near 06 UTC, nor the S_2 periodicity are well captured. At Malindi the diurnal cycle is peaking in the morning at 08 UTC (~11 LT) throughout the year (Figure 4d), with smaller values in phase with those observed at N'Koltang. Both stations are located near the Equator, and this feature might be linked to the passages of the ITCZ. The diurnal cycle from ERA40 (Figure 4h) is in good accordance with the observed one, though its magnitude is slightly underestimated.

5. Conclusion

[8] We have shown that PWV exhibits significant variability in a broad range of timescales over Central and West Africa and that GPS data are capable of capturing it. At the larger timescales, such as the seasonal cycle and intra-seasonal variability (3–50 days), variations in PWV from ERA40 (and ECWMF operational analysis) and GPS are in good agreement. Contrasted seasonal variations in PWV are illustrated at four GPS sites. Maxima are observed during the warm wet seasons, as a result of large-scale moisture transport. The most significant seasonal cycle is observed at Dakar with monthly-mean values ranging from ~15 in January to 50 kg m^{-2} in August. Intra-seasonal variability at this station shows roughly two modes: a winter mode with intense low-frequency modulations (reaching 20 kg m^{-2} over 2 days) and a summer mode with faster, though intense too, modulations (reaching 10 kg m^{-2} over 1 day). It has been shown that these modulations are correlated with the passage of equatorial waves and AEWs. The activity of these waves is different depending on the season. Equatorial waves are more intense during winter, while AEWs occur mainly during the monsoon season. The impact of these waves on PWV likely occurs via a modulation in horizontal moisture convergence, which may involve scale interactions with convection. The diurnal cycle in PWV is also illustrated at four GPS sites. Significant modulations are observed from GPS data, at three sites, with monthly-mean anomalies reaching ±1.5 kg m^{-2} during the wet seasons. The diurnal phase and the seasonal maximum both depend on geographical location. A S_2 component in PWV is also observed at the equatorial stations. Sub-monthly variability peaks in the evening for all sites, probably in connection with the maximum in convection observed over land. The diurnal cycle in PWV represented in ERA40 shows significant differences with GPS at all four sites, which confirms the weaknesses in the treatment of physical parameterizations in global circulation models [*Yang and Slingo*, 2001; *Tian et al.*, 2004]. The present work delineates limitations in the use of NWP models at this time scale. More generally, substantial work is needed to understand the relationship between humidity in the atmospheric column, surface evaporation fluxes and convection at this timescale. Finally, these results give good confidence into the quality and potential of GPS PWV estimates in Africa. New stations will be installed in the framework of the AMMA project (http://www.amma-international.org/) for the study of the water cycle and WAM dynamics.

[9] **Acknowledgments.** GPS ZTD data are from SOPAC archive (ftp://garner.ucsd.edu/pub/troposphere/). ERA40 reanalyses and ECMWF analyses are from the IPSL archive. Wavelet software was adapted from C. Torrence and G. Compo (original available at http://atoc.colorado.edu/research/wavelets/).

References

Bevis, M., S. Businger, S. Chiswell, T. A. Herring, R. A. Anthes, C. Rocken, and R. H. Ware (1994), GPS meteorology: Mapping zenith wet delay onto precipitable water, *J. Appl. Meteorol.*, *33*, 379–386.

Bock, O., M.-N. Bouin, A. Walpersdorf, J. P. Lafore, S. Janicot, and F. Guichard (2007), Comparison of GPS precipitable water vapour to independent observations and Numerical Weather Prediction model reanalyses over Africa, *Q. J. R. Meteorol. Soc.*, in press.

Diedhiou, A., S. Janicot, A. Viltard, P. de Felice, and H. Laurent (1999), Easterly wave regimes and associated convection over West Africa and tropical Atlantic: Results from the NCEP/NCAR and ECMWF reanalyses, *Clim. Dyn.*, *15*, 795–822.

Fontaine, B., P. Roucou, and S. Trzaska (2003), Atmospheric water cycle and moisture fluxes in the West African monsoon: Mean annual cycles and relationship using NCEP/NCAR reanalysis, *Geophys. Res. Lett.*, *30*(3), 1117, doi:10.1029/2002GL015834.

Gendt, G. (2004), Report of the tropospheric working group for 2002, in *IGS 2001–2002 Technical Report*, *JPL Publ. 04-017*, pp. 209–212, Jet Propul. Lab., Pasadena, Calif.

Matthews, A. (2004), Intraseasonal variability over tropical Africa during northern summer, *J. Clim.*, *17*, 2428–2440.

Simmons, A. J., and J. K. Gibson (2000), The ERA-40 project plan, *ERA40 Proj. Rep. Ser. 1*, 62 pp., Eur. Cent. for Medium-Range Weather Forecasts, Reading, U. K.

Sultan, B., S. Janicot, and A. Diedhiou (2003), West African monsoon dynamics. part I: Documentation of intraseasonal variability, *J. Clim.*, *16*, 3389–3406.

Tian, B., B. J. Soden, and X. Wu (2004), Diurnal cycle of convection, clouds, and water vapor in the tropical upper troposphere: Satellites versus a general circulation model, *J. Geophys. Res.*, *109*, D10101, doi:10.1029/2003JD004117.

Wagner, T., S. Beirle, M. Grzegorski, S. Sanghavi, and U. Platt (2005), El Niño induced anomalies in global data sets of total column precipitable water and cloud cover derived from GOME on ERS-2, *J. Geophys. Res.*, *110*, D15104, doi:10.1029/2005JD005972.

Wheeler, M., and G. Kiladis (1999), Convectively coupled equatorial waves: Analysis of clouds and temperature in the wavenumber-frequency domain, *J. Atmos. Sci.*, *56*, 374–399.

Yang, G. Y., and J. Slingo (2001), The diurnal cycle in the tropics, *Mon. Weather Rev.*, *129*, 784–801.

O. Bock, IPSL, SA, Université Paris VI, 4, place Jussieu, F-75252 Paris cedex, France. (olivier.bock@aero.jussieu.fr)

M.-N. Bouin, LAREG, IGN, 6 et 8, av. Blaise Pascal, F-77455 Marine la Vallee, France.

F. Guichard and J. P. Lafore, GMME, CNRM, Météo-France, 42, av. Gaspard Coriolis, F-31957 Toulouse Cedex 01, France.

S. Janicot and B. Sultan, IPSL, LOCEAN, Université Paris VI, 4, place Jussieu, F-75252 Paris Cedex 05, France.